# Neutron and Gamma Ray Imaging for Nuclear Materials Identification

James A. Mullens
John Mihalczo
Philip Bingham
*Oak Ridge National Laboratory*
*Oak Ridge, Tennessee 37831-6010*
*865-574-5564*

## *Abstract*

This paper describes tomographic imaging capabilities for fissile object identification. The tomographic capabilities add object spatial and material properties information that result in a more detailed item signature (template) and provide more information for physical attributes analyses. One method of examining fissile objects in sealed containers is through a radiation signature acquired by shining a $^{252}$Cf or DT generator source through the container and measuring the resulting radiation at detectors on the other side. This measurement gives a gamma and/or neutron radiation transmission profile of the object, mixed with the radiation produced by the induced fissions in any fissile materials.

Whereas the method above measures the fissile object at a single position, tomography images the interior of an item by making transmission measurements from all angles around the object. The advantage is more geometric and materials property information. The tomographic image provides more information about the geometry of the object, which should lead to better interpretation of the radiation signature. Interrogating with both gamma rays and neutrons of varying energies allows the system to construct separate tomographic views of the object's approximate gamma and neutron interaction properties (cross sections). The combination of geometric and materials property information will result in better template matching and attributes analysis.

The paper presents Monte Carlo simulations illustrating this technique.

## *Introduction*

This paper describes a tomographic imaging capability designed for use with the existing Nuclear Materials Inspection System (NMIS). NMIS measures a variety of radiation signatures: 2$^{nd}$ order correlations (2 detector, time-dependent coincidences), 3$^{rd}$ order correlations, and multiplicities [2]. NMIS can measure actively using a radiation source or passively using the unknown target's own radiation. It measures radiation arrival with 1 ns precision so it is capable of measuring fast (metal) fissile targets. The system can use as many as 10 detectors and calculate the coincidences among any pair or triplet of these detectors.

We intend for the imaging capability to complement these other measurements. The desired image resolution is on the order of 1 cm, which seems appropriate considering the free path length of neutrons in fissile materials. The image can be made from high-energy gamma ray and/or neutron interrogation of the unknown target. We expect the imaging capability to add geometric information about an unknown item being measured, and allow more precise interpretation of the signatures which NMIS currently measures. An image also has its own value in that the operator can relate to it naturally. We expect that the imaging will also benefit by the information in the existing NMIS signatures and thereby make the image more precise.

This paper uses a simple example problem to illustrate the concept. The simulation results in this paper were produced using MCNP-PoliMi [3], a modification of MCNP 4.3c to NMIS measurement modeling. Simulations have been valuable in developing insights about the physical processes taking place in these measurements.

We first described the concepts for this measurement in a technical report [1]. That report covers some topics in more detail than this paper.

## *Measurement System Configurations*

There are two sources and one detector configuration used in these measurements. One source is a deuterium-tritium (DT) 14.1 MeV neutron generator with associated alpha detector. An alpha particle is emitted 180° from the direction of the generated neutron. By limiting the alpha detector's solid angle the alpha detector will pulse only when the neutron is emitted towards the detectors[i]. This is shown in Figure 1. The second source is $^{252}$Cf, a fission source that emits several neutrons and gamma rays per fission. Both sources are timed: the measurement computer receives a pulse each time a DT neutron is emitted towards the detectors or a $^{252}$Cf fission occurs. However, the $^{252}$Cf fission radiation is isotropic and there is no indication of direction to the measurement computer.

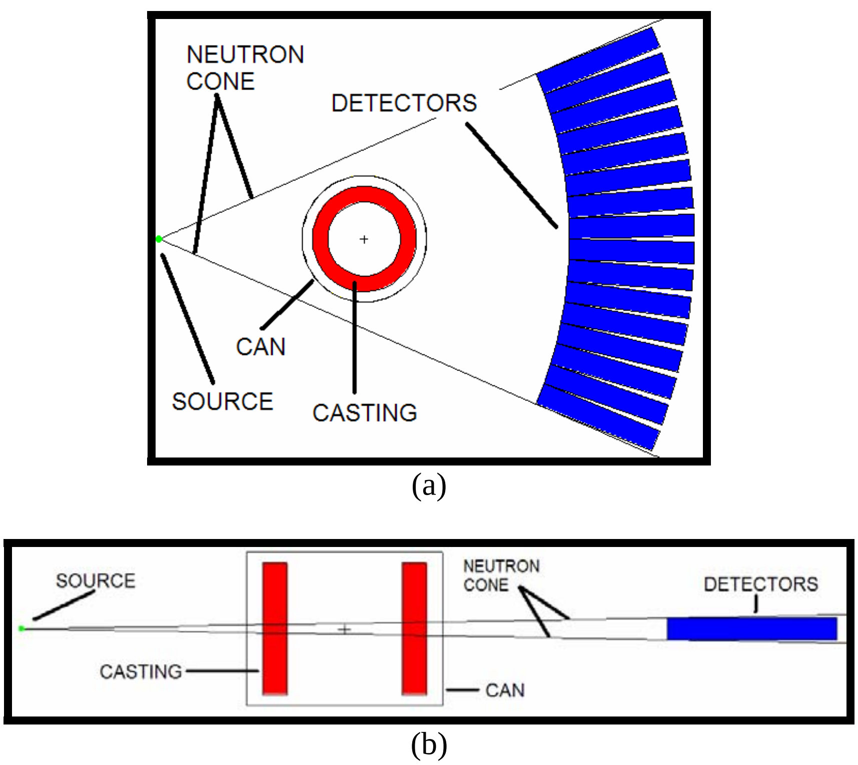


**Figure 1 Overhead (a) and side (b) views of measurement configuration and DT neutron emission cone.**

The detectors are shown in Figure 1 as an array of 16 1x1x6” detectors. This array covers the angle required by the imaging and results in an image resolution of about 1.3 cm. In practice 4 or 8 detectors would be used so that every 2$^{nd}$ or 4$^{th}$ position would have a detector; the gaps between the detectors lower the amount of cross talk between them. The measurement is made in steps by shifting the actual detectors into the gap positions until all detector positions have been measured. These are fast plastic scintillation detectors with a threshold that corresponds to 1 MeV neutrons and 0.125 MeV gamma rays. The distance between the source and the casting center is 25 cm; the distance between the source and detector faces is 48.7 cm.

The castings for these simulations are a standard size used to store highly-enriched uranium (HEU). These are right circular cylinders with outer diameter 12.7 cm, inner diameter 8.9 cm, and height 15.1 cm. A thin-walled steel can with diameter 15.1 cm and height 17.8 cm surrounds the casting. Simulated measurements are made with castings of different materials: HEU, 60% enriched U, natural U, steel, and aluminum. The HEU casting is the reference standard to which the other casting materials are compared.

A second series of castings adds a plastic rod to the castings just described. This rod is located at the center of the casting. It has the same height as the casting and a diameter of 4 cm (roughly half of the interior diameter of the casting). The figure labels for these castings are the material name followed by ‘P’.

All castings are radially symmetric to minimize the amount of MCNP-PoliMi simulation time required. The measurement can be done with just one projection (one measurement as shown in Figure 1, without measurements of additional rotations of the casting). An image measurement of a significantly non-symmetric target requires measurements for “all rotations” of the target, where each measurement is called a *projection*. The angular step should be about 1 detector’s width (2.7°), which is 132 projections. However, there are specialized methods of image reconstruction that apply to our circumstances (regular geometric shapes of machined parts) that vastly reduce the number of projections required. (We do not discuss these in this paper.)

Correlations and images, described below, are measured at the same time. If multiple imaging projections are measured, the correlations would be summed over all projection measurements. The simulations shown in the following sections are highly converged. The time spent measuring a projection is 12 seconds for a $^{252}$Cf source ($5\times10^6$ fissions per second from 5 μ-grams) or a DT generator (operating at $10^8$ neutrons per second, where the neutrons per second emitted in the cone is $0.42\times10^6$). This duration was required to converge the correlation signatures. Other simulations for thicker targets have found that a good image is obtained in 4 seconds for the DT generator. We expect that, should a full tomographic scan be required by the circumstances, the measurement time would be about 132 projections × 4 seconds/projection = 9 minutes. Since the correlations are summed across all projections this would yield 530 seconds of correlation measurement as opposed to the 12 seconds used in this report.

## ***Correlation Signatures***

The correlation signature measures coincidence between the source and the detectors, as a function of time after source emission. This is shown in Figure 2 for the DT generator simulation. (All correlations are normalized by the number of source counts measured.) The arrival of radiation is similar for all materials: at about 7 ns gamma rays produced by neutron interactions with the casting arrive; at 10 ns the uncollided neutrons arrive; subsequently additional gamma rays and neutrons arrive from continued interaction with the casting. The fissionable/fissile materials produce induced fission radiation that is apparent here after 15 ns after the source emission. The simulations for castings with the additional plastic rod are shown as dotted lines. The main effect of the rod is more attenuation of the source neutrons, which arrive at 10 ns.

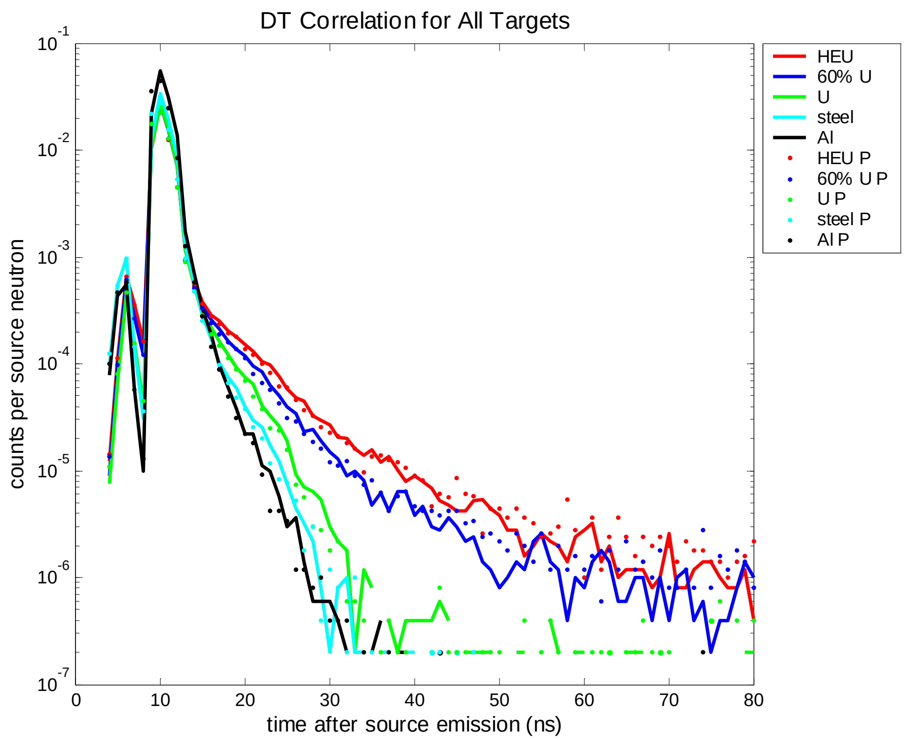


**Figure 2 Correlations for the DT generator measurement simulation.**

The correlations shown are the sum of all correlations from the detectors in the casting's shadow. The correlations are measured separately for all detectors, but the summation's purpose is to measure the sparse amount of induced radiation that arrives after 15 ns. All detectors can be summed because the spatial (detector) dependence of this induced fission radiation is weak because it is isotropic.

The $^{252}$Cf correlation simulations are different due to the fact that gamma rays and neutrons are emitted with fission energy spectra. These correlations are shown in Figure 3. The arrival of radiation is similar for all materials: at about 2 ns the uncollided source gamma rays arrive at the detectors; at 10 ns gamma rays from the source neutron interaction with the casting arrives in substantial numbers; uncollided source neutrons arrive between 10 ns, through 40 ns, and beyond; radiation from neutron interactions with the casting arrives in the same period of time. The fissile materials produce induced fission radiation that is most apparent here after 40 ns. There is a complication, however, that obscures the induced fission radiation. The $^{252}$Cf source is also a source of slightly-delayed fission gamma rays. The detectors see these gamma rays through the shielding that the casting provides. Thus the steel and aluminum casting measurements observe late gamma rays that are comparable to the number produced in uranium castings since the uranium castings shield the $^{252}$Cf source heavily while producing their own fission gamma rays. The main effect of the plastic rod is more attenuation of the source neutrons which arrive mainly between 10 and 40 ns.

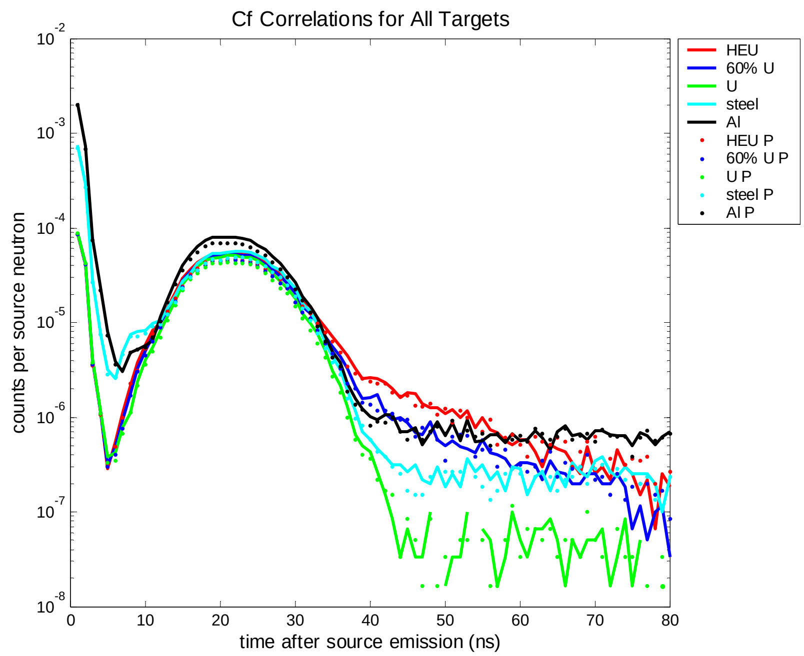


**Figure 3 Correlations for the Cf source measurement simulation.**

In order to illustrate unknown target identification, a set of features is extracted from the correlation measurements. Features selected for the DT measurements are:

- Attenuation of the 14.1 MeV neutrons by the target through rate of arrival at 10 ns.
- Generation of gamma rays by 14.1 MeV neutrons at the target through rate of arrival between 3 and 7 ns. These counts are approximately the inelastic and induced fission gamma rays.
- High-energy neutron interaction with the target, measured through rate of arrival between 14 and 29 ns. These counts reflect the single scatterings and fissionable materials fissions in the target.
- Radiation due to neutron interactions with the target, measured through the rate of arrival between 30 and 69 ns. These counts reflect multiple scatterings and induced fission in the target.

Features selected for the $^{252}$Cf measurements are:

- Attenuation of the source gamma rays by the target through rate of arrival at 2 ns.
- Attenuation of the source neutrons by the target through rate of arrival between 12 and 29 ns. This arrival time corresponds to source neutrons with energy between 1.5 and 8.6 MeV. This time the is the peak of the neutron arrivals where the source neutrons are expected to dominate the counts. This feature can be subdivided into a feature for different arrival time ranges, as follows.
- Attenuation of the higher-energy source neutrons by the target through rate of arrival between 12 and 15 ns (5.5 MeV to 8.6 MeV).
- Attenuation of the mid-energy source neutrons by the target through rate of arrival between 16 and 29 ns (1.5 MeV to 4.8 MeV).

Attenuation features are taken only from the detectors that are in the target's shadow. Attenuation values are calculated by comparison to a calibration measurement in which the same detector configuration is used but there is no target. The log of the ratio to the calibration measurement is proportional to target cross section × density (actually, the integral of this quantity on the line between the source and the detector).

## *Image Signatures*

The images are reconstructed through the attenuation features of the measured correlations. The geometric (per detector) distribution of these attenuations is used. The simulation of a typical measurement is shown in Figure 4. The attenuation due to the HEU casting walls and the hollowness of the interior is evident. The shape is not evident when a more complex object is measured.

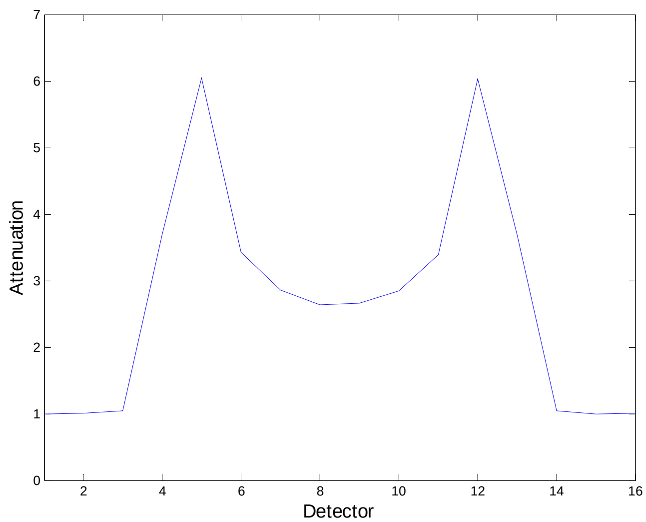


**Figure 4 14.1 MeV neutron attenuation by a HEU casting as seen by each detector in the array.**

The images constructed for this report are:

- A 14.1 MeV neutron attenuation image from the DT measurement.
- A gamma fission spectrum attenuation image from the $^{252}$Cf measurement.
- A fission spectrum neutron attenuation image across the range of 1.5 to 8.6 MeV, from the $^{252}$Cf measurement.
- A fission spectrum neutron attenuation image across the range of 5.5 to 8.6 MeV, from the $^{252}$Cf measurement.
- A fission spectrum neutron attenuation image across the range of 1.5 to 4.8 MeV, from the $^{252}$Cf measurement.

Tomographic image reconstruction is done through the simple and fast method: *filtered backprojection*. The aluminum casting with the plastic center rod is shown as an example because it most clearly shows the rod and casting together (Figure 5). Naturally, the images are blurred due to the limited image resolution used to minimize the number of detectors required. The rod is visible in the $^{252}$Cf neutron images and the DT neutron images. It is not visible in the $^{252}$Cf gamma images.

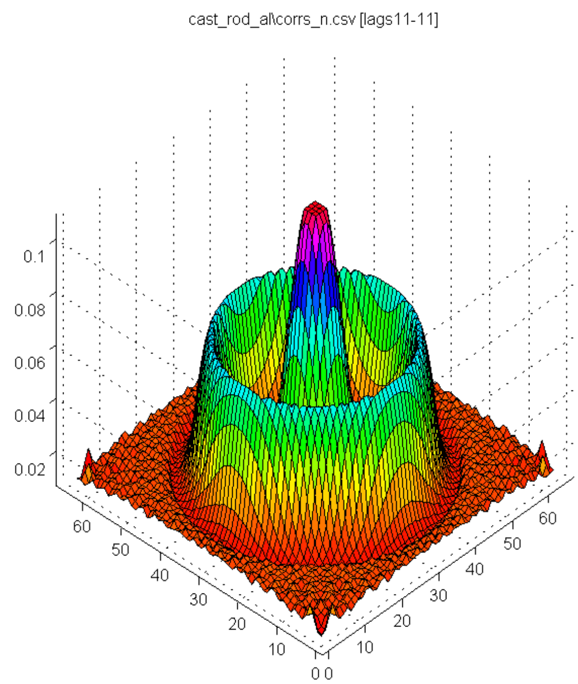


**Figure 5 Image of aluminum casting with plastic center rod using DT generator. The image shows the attenuation of 14.1 MeV neutrons over a two dimensional slice through the center of the casting. The x and y axis units are image pixel number. The z axis is log(attenuation).**

An intriguing result is a plot of log(attenuation) for gamma rays versus neutrons for every pixel in the image, using the $^{252}$Cf measurement. The gamma rays and neutrons have a fission energy spectrum in this case. This result appears in Figure 6 for all castings with the center plastic rod. Because of the casting's radial symmetry, each casting's result appears to follow a trajectory in this plot. The trajectory moves along the radius from the outside of the casting to the center. All trajectories start in the lower left corner, outside the casting, proceed to the casting wall (upper right) where it reverses direction, into the void between the wall and the center rod, and finally end at the center of the plastic rod.

The three uranium castings have very similar results. The steel and aluminum castings have a different ratio of gamma to neutron attenuation as can be seen by the different slope for their results. The neutron attenuation values (extreme right) are close for steel and uranium; the gamma ray attenuation values (vertical axis) are distinct for all three materials. The plastic is nearly invisible to the Cf gamma rays so the gamma attenuation value found is not precise.

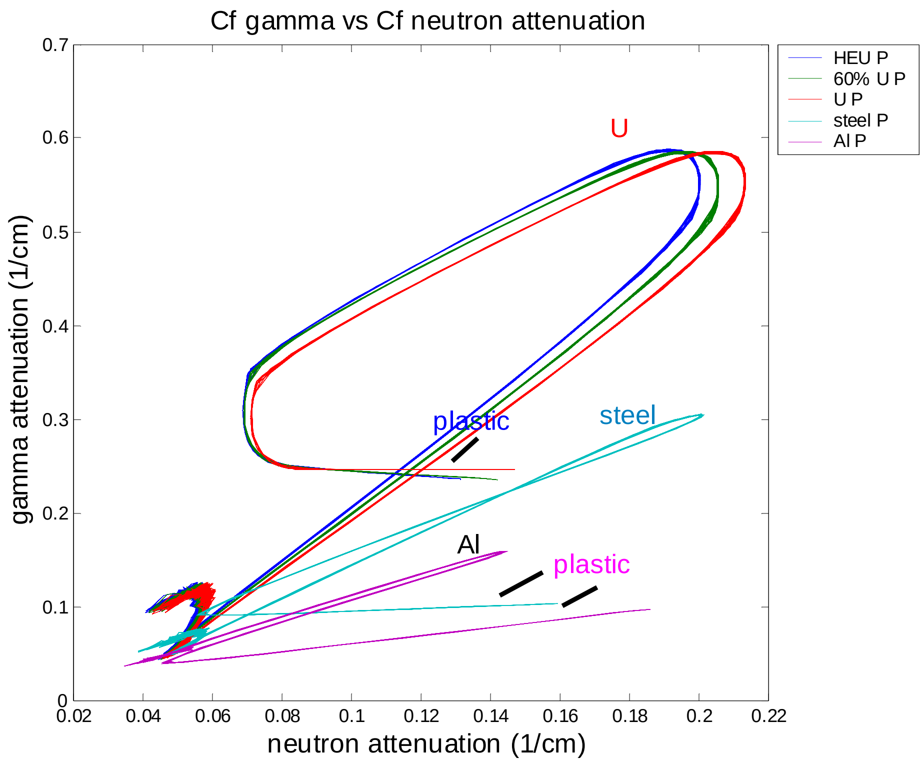


**Figure 6 Gamma image vs neutron image attenuation measured for each pixel in the image. Conveniently, these values appear to follow a trajectory because of the radial symmetry of the casting.**

## *Feature Selection*

The features described above and the log of the attenuation features were evaluated by a simple feature selection process. All 15 features were normalized to the range 0..1. The distance in feature space between all pairs of castings measured, in all possible feature spaces from dimension 1 to 15, was calculated. The overall best feature set was found using the criteria that the distance between any pair of castings should be maximized, that is, the minimum distance between any pair of castings was maximized. The distance for feature spaces of dimension N was normalized by $N^{1/2}$ so that it was proportional to the maximum distance possible in that feature space. Figure 7 shows, as an example, the 10 castings plotted in a 2D feature space. These features were the best *pair* of features found through the evaluation process above.

The best feature set consisted of:

- DT high energy neutron interactions,
- DT fissile (delayed) radiation,
- Log($^{252}$Cf source neutron attenuation),
- $^{252}$Cf neutron image variation, and
- $^{252}$Cf gamma image variation.

The DT generator features in this list are nearly always selected in feature subsets. The $^{252}$Cf high-energy neutron image feature is also frequently selected in feature subsets.

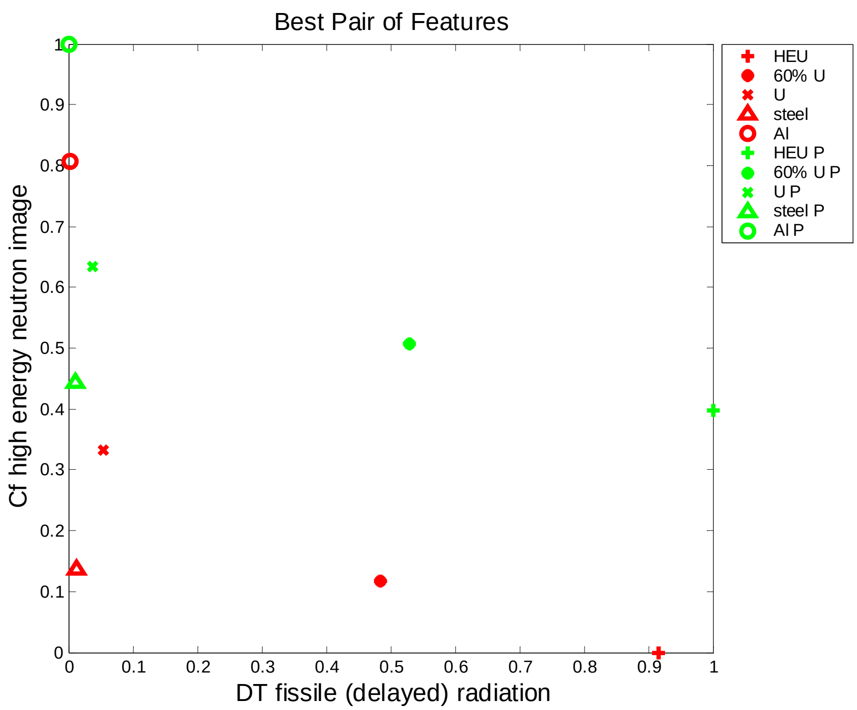


**Figure 7 An example of 2D feature space (feature pairs).**

This result is, of course, specific to the targets measured here. However this suggests that a combination of correlation and image features can be optimum to distinguish an unknown target from a reference target.

This example application selects those features that give the best contrast between the castings measured. A selected feature set gives the best chance of distinguishing one casting from another, in the sense of matching (classifying) an unknown target. If the goal was instead to quantitatively relate the casting's physical attributes (mass, enrichment, materials, and density) to the measurement results, the selected feature set would still be a good choice since these are the features most sensitive to the castings' differences.

## *Conclusions*

A detector array gathers spatial radiation information, and tomographic imaging is one way to use this information. Images and correlations provide complementary information about an unknown target. Images are particularly sensitive to the geometry of the target; correlations are more sensitive to the fissile characteristics. Knowledge of an unknown target's interior geometry will help in interpreting the correlation measurements, and *vice versa*.

We think that the DT generator is the overall best source to use, but these results show that the images produced by the $^{252}$Cf source are also useful. The $^{252}$Cf gamma ray interrogation complements neutron interrogation (see Figure 6) and can help to distinguish different materials.

Some image reconstruction problems remain. These arise from the complicated interaction of neutron and high-energy gamma rays with the target: forward scattering, inelastic scattering, fission, and other effects. In general this requires a more detailed interaction model be used in the reconstruction algorithm. The measurement system might minimize the modeling required by employing neutron-gamma discrimination (pulse shape discrimination) and detector pulse height discrimination (incident particle energy discrimination).

## *References*

1. Mullens, J. A., "Addition of Tomographic Capabilities to NMIS", March 2003, Report No. Y/LB-16160, Y-12 National Security Complex.
2. J. T. Mihalczo, J. A. Mullens, J. K. Mattingly, and T. E. Valentine, "Physical Description of Nuclear Materials Identification System (NMIS) Signatures," Nuclear Instruments & Methods in Physics Research A, 450 (2000) 531-555.
3. S.A. Pozzi, E. Padovani, and M. Marseguerra, "MCNP-PoliMi: A Monte Carlo Code for Correlation Measurements," Nuclear Instruments and Methods in Physics Research A, 513/3 pp. 550-558.

---

[i] Paul Hausladen, ORNL, pointed out that the neutron emission cone need not to be limited to geometric cone as has been used with DT generators. It can be any shape that best matches the detector array. This substantially improves the measurement for complex objects with three dimensional geometry.